Novel image fusion method based on discrete fractional random transform

Qing Guo (郭 擎) and Shutian Liu (刘树田)*

Department of Physics, Harbin Institute of Technology, Harbin 150001, China

**E-mail: stliu@hit.edu.cn*

Received December 8, 2009

We introduce a new spectrum transform into the image fusion field and propose a novel fusion method based on discrete fractional random transform (DFRNT). In DFRNT domain, high amplitude spectrum (HAS) and low amplitude spectrum (LAS) components carry different information of original images. For different fusion goals, different fusion rules can be adopted in HAS and LAS components, respectively. The proposed method is applied to fuse real multi-spectral (MS) and panchromatic (Pan) images. The fused image is observed to preserve both spectral information of MS and spatial information of Pan. Spectrum distribution of DFRNT is random and uniform, which guarantees that good information is reserved.

OCIS codes: 100.0100, 280.0280, 330.0330, 070.0070.

doi: 10.3788/COL20100807.0656.

Image fusion involves combining multiple images of the same scene with complementary information to generate a new composite image with more information and better quality than the individual image obtained solely by a single sensor. In remote sensing, multi-spectral (MS) images sufficient spectral information but poor spatial resolution, while panchromatic (Pan) images are marked by high spatial resolution but low spectral information. In this letter, we aim to achieve pixel-level fusion of MS and Pan images to preserve spectral information while enhancing spatial details, which can better serve applications such as land classification and road detection.

There are various fusion algorithms at the pixel level, including intensity-hue-saturation (IHS), Brovey, wavelet, and contourlet transforms[1−5]. IHS method transforms three MS bands from red-green-blue (RGB) space into IHS space to separate spatial information from spectral components. After replacing intensity with Pan, the merged result is converted back into RGB space. Although this method can preserve high spatial resolution, it distorts spectral information[6]. Brovey fusion is a simple color normalized method that commonly introduces spectral distortion. In the contourlet method, down-sampling and up-sampling processes prompt contourlet transform to lose translation invariance and further introduce the Gibbs effect in the resultant image.

For wavelet methods, the Pan and each band of MS images are decomposed into an approximation and a set of detailed images. Band by band, the approximation image from MS is combined with details from Pan. Then, inverse wavelet transform is performed to obtain the fused images. This method can obtain sound fusion results; however, the wavelet decomposition level produces an impact on fusion performance. If the decomposition level is low, fused images preserve more spectral characteristics but fail to preserve spatial details appropriately. With a higher level of decomposition, the performance of spatial details gradually increases; however, the spectral information cannot be preserved very well as low frequency coefficients are decomposed repeatedly.

IHS and Brovey transforms are direct conversions between pixel values of images, while wavelet transform is a joint space-frequency transform. Wavelet coefficients straightly display approximate and detailed spatial images corresponding to original image. These types of representations are marked by incompleteness and uncertainty. Although wavelet has space and frequency information, it has no exact transform domain. Two-dimensional (2D) wavelet bases are isotropic and have limited directional representations of image details. It is noted that Fourier transform (FT) and fractional Fourier transform (FrFT) are joint space-frequency transforms. Their transform coefficients represent the contribution of each basis function at each frequency, thus they have exact transform domains. They can show the transform spectrum, and spatial image can be obtained only after inverse transform. FT and FrFT clearly display the features of signals in frequency domain, which is difficult to display in the spatial domain. Their kernel functions allow the perfect frequency resolution to be obtained, as the kernel per se is a window of infinite length. FT and FrFT convert grayscale distribution of an image into its frequency distribution, and frequency indicates the extent of change in gray scale. Therefore, performing fusion in such transformed domains is an indirect change of the original image simultaneously based on space image features and different spectrum distribution features.

In this letter, we propose a novel fusion method based on discrete fractional random transform (DFRNT)[7]. DFRNT originates from discrete fractional Fourier transform (DFrFT)[8]. It features excellent mathematical properties inherited from FrFT, in addition to a number of special spectrum distribution features of its own. The randomness of DFRNT can randomly distribute the changed information by fusion, which introduces lower influence than same-strength changes at the concentrated location in spectra. This ensures less spectral distortion. The uniformity of DFRNT ensures majority of acceptable fusion results when distortions occur in any position of the spectrum; this lends certain robustness to the method. In the DFRNT domain, a nominal high-frequency component with spatial details and a nomi-

nal low-frequency component with spectral information can be extracted. For different frequency components, different fusion rules are utilized according to different fusion goals. Furthermore, at half periodicity, DFRNT produces real output for a real signal, which can save storage space for image data, offering convenience for storage, compared with the complex output.

For discrete transforms, kernel matrix is key. It can be expressed as the product of eigenvector and eigenvalue matrices through eigendecomposition. Meanwhile, DFRNT and DFrFT ultimately originate from discrete Fourier transform (DFT). Eigendecomposition of DFT are a set of Hermite-Gaussian functions, which are eigenfunctions of continuous FT. The FT is usually defined as

$$X(\omega)=\frac{1}{\sqrt{2\pi}}\int_{-\infty}^{\infty}x(t)\exp(-\mathrm{i}\omega t)\mathrm{d}t,$$
$$x(t)=\frac{1}{\sqrt{2\pi}}\int_{-\infty}^{\infty}X(\omega)\exp(\mathrm{i}\omega t)\mathrm{d}\omega. \quad (1)$$

Complex exponential (sines and cosines) functions as basis functions are orthogonal. For conventional DFT, elements of DFT kernel matrix $\mathbf{F}$ are defined by

$$\mathbf{F}_{nk}=\frac{1}{\sqrt{N}}\exp\left(-\mathrm{i}\frac{2\pi kn}{N}\right),\ 0\le n,k\le N-1, \quad (2)$$

where N pertains to element numbers (i.e., there are N elements in the input vector for conventional DFT). Kernel matrix of DFT has four eigenvalues: $\{1,\ -\mathrm{i},\ -1,\ \mathrm{i}\}$. For DFT eigenvectors, any linear combinations with the same eigenvalues remain DFT eigenvectors. To avoid ambiguity in deciding eigenvectors, a commuting matrix $\mathbf{S}$ ($\mathbf{SF}$=$\mathbf{FS}$) is introduced to compute eigenvectors of $\mathbf{F}$. $\mathbf{S}$ is defined as

$$\mathbf{S}=\begin{pmatrix}2 & 1 & 0 & 0 & \cdots & 0 & 1\\ 1 & 2\cos\omega & 1 & 0 & \cdots & 0 & 0\\ 0 & 1 & 2\cos 2\omega & 1 & \cdots & 0 & 0\\ \vdots & \vdots & \vdots & \ddots & \vdots & \vdots & \vdots\\ 1 & 0 & 0 & 0 & \cdots & 1 & 2\cos(N-1)\omega\end{pmatrix}, \quad (3)$$

where $\omega=2\pi/N$. As a result of commutative property, $\mathbf{S}$ and $\mathbf{F}$ have the same eigenvectors, though they correspond to different eigenvalues. As $\mathbf{S}$ is a symmetric matrix, its eigenvectors are all real and orthonormal to one another. These eigenvectors construct an orthonormal basis, which plays the same role as Hermite function in the continuous case. Thus, eigendecomposition of DFT kernel matrix $\mathbf{F}$ is written as

$$\mathbf{F}=\sum_{k\in E_0}\mathbf{v}_k v_k^{\mathrm{t}}+\sum_{k\in E_1}(-\mathrm{i})\mathbf{v}_k v_k^{\mathrm{t}}+\sum_{k\in E_2}(-1)\mathbf{v}_k v_k^{\mathrm{t}}+\sum_{k\in E_3}(\mathrm{i})\mathbf{v}_k\mathbf{v}_k^{\mathrm{t}}, \quad (4)$$

where superscript t denotes the transpose, E_0 is a set of indices for eigenvectors v_k belonging to eigenvalue $\lambda_k=1$, E_1 for $\lambda_k=-\mathrm{i}$, and so on. DFT has several mathematical properties, including linearity ($\mathbf{F}(ax_1+bx_2)=a\mathbf{F}x_1+b\mathbf{F}x_2$), multiplicity ($T=4$), and Parseval's energy conservation $\left(\sum_{n=0}^{N-1}|x(n)|^2=\frac{1}{N}\sum_{k=0}^{N-1}|X(k)|^2\right)$. Spectrum energy is usually highly concentrated at the origin of the DFT coefficients matrix, which introduces large distortion when performing fusion within.

For the FrFT, transform kernel is defined as

$$K_\theta(v,u)=\sqrt{\frac{1-\mathrm{i}\cot\theta}{2\pi}}\exp\left[\mathrm{i}\frac{(v^2+u^2)\cos\theta-2uv}{2\sin\theta}\right]=\sum_{n=0}^{\infty}\exp(-\mathrm{i}n\theta)h_n(v)h_n(u), \quad (5)$$

where $h_n(\cdot)$ is the nth order normalized Hermite-Gaussian function. Equation (5) provides an eigendecomposition of continuous FrFT kernel, and illustrates that eigenvectors of FrFT are Hermite functions. As FrFT possesses the same eigenfunction as FT, eigenvectors $\{\mathbf{v}_\alpha^j\}(j=1,2,\cdots,N)$ of DFrFT can be calculated through $\mathbf{S}$, as defined in DFT. Thus, $\{\mathbf{v}_\alpha^j\}$ forms an orthonormal basis equivalent to Hermite-Gaussian polynomials in continuous FrFT. Then, $N\times N$ eigenvector basis matrix $\mathbf{V}_\alpha$ is obtained as $\mathbf{V}_\alpha=[\mathbf{v}_\alpha^1\mathbf{v}_\alpha^2\cdots\mathbf{v}_\alpha^N]$. In the calculation, DFT-shifted version of $\{\mathbf{v}_\alpha^j\}$ is needed. From Eq. (5), eigenvalue of FrFT can be written as $\lambda_k=\exp(-\mathrm{i}\alpha k\pi/2), k=0,1,2,\cdots,\infty$, where α is the fractional order. In DFrFT, eigenvalues remain unchanged, with only limited numbers (i.e., $k=0,1,2,\cdots,N$). These eigenvalues construct a diagonal matrix $\mathbf{D}_\alpha$ as

$$\mathbf{D}_\alpha=\begin{cases}\mathrm{diag}(1,\mathrm{e}^{-\mathrm{i}\alpha\pi/2},\cdots,\mathrm{e}^{-\mathrm{i}\alpha(N-1)\pi/2}),\\ \qquad N\text{ is odd}\\ \mathrm{diag}(1,\mathrm{e}^{-\mathrm{i}\alpha\pi/2},\cdots,\mathrm{e}^{-\mathrm{i}\alpha(N-2)\pi/2},\mathrm{e}^{-\mathrm{i}\alpha N\pi/2}),\\ \qquad N\text{ is even}\end{cases}. \quad (6)$$

In $\mathbf{D}_\alpha$, there is a jump in the last eigenvalue for even N. Such assignments of eigenvalues are consistent with the multiplicity rule in DFT. Based on $\mathbf{V}_\alpha$ and $\mathbf{D}_\alpha$, kernel transform of DFrFT is defined as

$$\mathbf{F}^\alpha=\mathbf{V}_\alpha\mathbf{D}_\alpha\mathbf{V}_\alpha^{\mathrm{t}}. \quad (7)$$

For one-dimensional (1D) signal $x(n)$, DFrFT can be expressed as $\mathbf{X}_\alpha(\mathbf{n})=\mathbf{F}^\alpha\mathbf{x}(\mathbf{n})$, and DFrFT is reduced into DFT with $\alpha=1$. As eigenvectors are orthonormal, $\mathbf{V}_\alpha\mathbf{V}_\alpha^{\mathrm{t}}=\mathbf{I}$ ($\mathbf{I}$ is the identity matrix) and $\mathbf{D}_{-\alpha}=\mathbf{D}_\alpha^*$. These confirm that DFrFT has the same properties as FrFT, including linearity, multiplicity, unitarity ($\mathbf{F}^{-\alpha}=(\mathbf{F}^\alpha)^*$), additivity ($\mathbf{F}^\alpha\mathbf{F}^\beta=\mathbf{F}^{\alpha+\beta}$), and energy conservation. DFrFT is a generalized fractional power form of DFT; its spectrum energy usually centralizes at low frequency, but with relative decentralization compared with DFT.

DFrFT has the same eigenvectors as DFT, but with fractional power eigenvalues. Meanwhile, DFRNT has the same eigenvalues as DFrFT, but with random eigenvectors. The whole generation process of DFRNT kernel matrix is roughly the same as that in DFrFT. The essence from DFrFT to DFRNT is to change $\mathbf{S}$ to a diagonal random symmetric matrix $\mathbf{Q}$, which introduces randomness of DFRNT. Matrix $\mathbf{Q}$ is generated by $N\times N$ real random matrix $\mathbf{E}$ with a relation of $\mathbf{Q}=(\mathbf{E}+\mathbf{E}^{\mathrm{t}})/\mathbf{2}$. Kernel matrix $\mathbf{R}^\alpha$ is defined in a commutative way that $\mathbf{R}^\alpha\mathbf{Q}=\mathbf{Q}\mathbf{R}^\alpha$. As $\mathbf{Q}$ is symmetric, eigenvectors

$\{\mathbf{V}'_{Rj}(j=1,2,\cdots,N)\}$ of $\mathbf{R}^{\alpha}$ are all real and orthonormal to one another. Then, $\{\mathbf{V}'_{Rj}\}$ is normalized to $\{\mathbf{V}_{Rj}\}$ using the Schmidt standard normalization procedure. Eigenvector matrix $\mathbf{V}_R$ is composed of N column vectors $\{\mathbf{V}_{Rj}\}$ obtained by $[\mathbf{V}_R]=[\mathbf{V}_{R1}\mathbf{V}_{R2}\cdots V_{RN}]$, where $\mathbf{V}_R\mathbf{V}_R^{\mathrm{t}}=\mathbf{I}$. It is noted that DFT-shift is not needed here, as eigenvectors are generated from a symmetrical random matrix. Coefficient matrix corresponding to eigenvalues of DFRNT is defined as

$$\mathbf{D}_{R\alpha}=\mathrm{diag}\left[1,\exp\left(-\mathrm{i}\frac{2\pi\alpha}{T}\right),\cdots,\exp\left(-\mathrm{i}\frac{2(N-1)\pi\alpha}{T}\right)\right], \tag{8}$$

where T indicates periodicity of DFRNT. Here, there is no jump for odd and even integer N. Thus, $\mathbf{R}^{\alpha}$ can be constructed as $\mathbf{R}^{\alpha}=\mathbf{V}_R\mathbf{D}_{R\alpha}\mathbf{V}_R^{\mathrm{t}}$. DFRNT for 1D and 2D signals can be written respectively as

$$\mathbf{X}_{R(\alpha)}(n)=\mathbf{R}^{\alpha}\mathbf{x}(n) \text{ and } \mathbf{X}_{R(\alpha)}=\mathbf{R}^{\alpha}\mathbf{x}(\mathbf{R}^{\alpha})^{\mathrm{t}}. \tag{9}$$

Eigenvectors of DFRNT depend on the random matrix $\mathbf{Q}$ (or $\mathbf{E}$). For different $\mathbf{E}$, DFRNT outputs will be different and always random. It should be noted that DFRNT output for a real signal becomes a real number when α is taken as $hT/2$, where h is an integer. As $\mathbf{D}_{R\alpha}$ is real in this case, $\mathbf{R}^{\alpha}$ is real as well. Real outputs can save storage space of image compared with the complex outputs.

DFRNT features excellent mathematical properties as DFrFT, in addition to its own random and uniform spectrum distribution features (i.e., its spectrum energy is dispersed uniformly). These properties may be comprehended directly from spectra of DFRNT and DFrFT, (Fig. 1). For DFrFT, a few high amplitudes are concentrated at the origin, and many extremely low, even zero, amplitudes are in other positions. In contrast, for DFRNT, the spectrum with different values spreads out, and many amplitudes can play roles in the fusion. Thus, it has a lower influence on the same-strength changes in spectra. This guarantees low spectral distortion. In DFrFT, when large distortion occurs at the origin, fusion results will be poor, and even the whole band information is lost. In the uniform DFRNT, majority of fusion results are acceptable, even distortion occurring at any position. The uniformity confirms certain robustness.

In this letter, MS and Pan images are registered before fusion. For each band, the proposed DFRNT fusion algorithm is summarized as follows.

Step 1: Low-resolution MS is interpolated to high-resolution Pan. Thus, MS is re-sampled to the same pixel size as Pan using cubic interpolation.

Step 2: Pan image is modified using histogram matching to allow its brightness and contrast to match that of each MS image, band by band. More precisely, after computing histograms of both Pan and each band MS images, the histogram of each band MS image is used as reference to which the histogram of Pan image is matched.

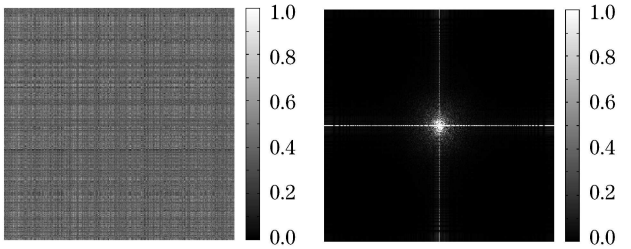

Fig. 1. Spectra of (a) DFRNT and (b) DFrFT for the 1st band of TM image.

Step 3: Pan and all bands of MS images are transformed to DFRNT domains.

Step 4: Substituting high-frequency component of MS using the details of Pan results in spectral loss. Meanwhile, discarding low-frequency component of Pan results in loss of spatial information. Fusion is performed at both high- and low-frequency components. Then, fusion results at these two components are combined to provide a high-resolution MS image. Weighted combination principle is adopted as the fusion rule. When the contribution of one image information is large, a large weight coefficient is employed to preserve information adaptively into the fused image without losing information of the other image. This is more scientific than merely selecting the main contributive information of one image. Furthermore, the weighted combination introduces less information loss of the original images.

In DFRNT domain, the high amplitude spectrum (HAS) component is the nominal low-frequency component. Meanwhile, the low amplitude spectrum (LAS) component is the nominal high-frequency component. As a rule, majority of spectrum energy is carried in the low-frequency component. In DFRNT, energy is calculated through sorted spectrum amplitudes in a descending order. Then, ratios of different parts of energy to the total energy are calculated to extract HAS/LAS components. When the ratio is extremely small, the LAS component predominates in the transform spectrum. Thus, the fusion result cannot preserve more spectral information. In contrast, the fusion result cannot improve spatial resolution properly. The ratio with the best vision and evaluation results as a whole serves as the separation threshold to extract the HAS/LAS components.

Step 5: For the HAS component, the fusion goal is to preserve spectral information as much as possible while adding spatial details of Pan into the MS image. To minimize spectral distortion, only individual characteristics of Pan are added to each corresponding MS band. The common characteristic of MS and Pan in the HAS component is

$$MP'_{\mathrm{HAS(com)}}=\min[M'_{\mathrm{HAS}},P'_{\mathrm{HAS}}], \tag{10}$$

where M'_{HAS} and P'_{HAS} are the HAS components of MS and Pan images, respectively. The individual characteristic of Pan in the HAS component is

$$P'_{\mathrm{HAS(own)}}=P'_{\mathrm{HAS}}-MP'_{\mathrm{HAS(com)}}. \tag{11}$$

To further reduce spectral distortion by adding more spatial information of Pan, individual characteristics of Pan

are weighted into the MS according to the contribution of Pan's information over total information. If the contribution is high, more spatial information of Pan is added to improve spatial quality. If the contribution is low, information of MS becomes the main portion. Thus, less spatial information of Pan is added to preserve spectral information as much as possible. Therefore, fused spectrum of the HAS component is obtained using

$$F'_{\mathrm{HAS}} = M'_{\mathrm{HAS}} + \frac{P'_{\mathrm{HAS}}}{M'_{\mathrm{HAS}} + P'_{\mathrm{HAS}}} P'_{\mathrm{HAS(own)}}. \quad (12)$$

Step 6: For the LAS component, the fusion goal is to improve spatial details of the fused image. In practice, two source images commonly provide useful information for fusion. If any part of any source image is discarded, it may introduce information loss of the fused image. Thus, the weighted combination rule is utilized in this letter. To add greater spatial information, high weight for Pan is performed when the contribution of Pan's information to the total information is low. For the same reason, low weight for MS is performed when the contribution of MS information to the total information is high. The weighted combination rule for each band is utilized as

$$F'_{\mathrm{LAS}} = \frac{P'_{\mathrm{LAS}}}{M'_{\mathrm{LAS}} + P'_{\mathrm{LAS}}} M'_{\mathrm{LAS}} + \frac{M'_{\mathrm{LAS}}}{M'_{\mathrm{LAS}} + P'_{\mathrm{LAS}}} P'_{\mathrm{LAS}}, \quad (13)$$

where M'_{LAS}, P'_{LAS}, and F'_{LAS} indicate LAS components of MS, Pan, and fused images, respectively.

Step 7: Fused image is obtained after taking inverse DFRNT for these fused spectrum bands.

Thematic mapper (TM) and Satellite Pour I'Observation de da Terra (SPOT) Pan images reflect considerable spectral variety. Color composite of TM bands 5, 4, and 1 in red, green, and blue (TM 541RGB) is selected for the illustration, as spectral range of these bands is extremely different from that of SPOT Pan. Thus, possible spectral distortion can be effectively tested. As TM band 4 displayed in green has the lower brightness compared with the other two bands, all TM bands are linearly stretched with a 99% clipping at both high and low ends of the image histograms. Such a stretch lends an effective use of the whole pixel value range (0–255 for 8-bit data). With all bands possessing the same pixel value range, high-quality color composite with rich and balanced colors is obtained to demonstrate if any subtle color distortion has been introduced.

Resolutions of TM and SPOT Pan images are 30 and 10 m, respectively. SPOT Pan and re-sampled TM (10 m) images are illustrated in Figs. 2(a) and (b). The fusion result (10 m) is presented in Fig. 2(c). The performance of DFRNT method is compared with the standard IHS method. To validate the features of DFRNT, the performance of DFRNT method is likewise compared with that in the DFrFT domain using the same fusion process. The results are presented in Figs. 2(d) and (e).

From these figures, it is observed that fused image using DFRNT preserves majority of spectral information of MS and improves spatial resolution. IHS method distorts certain spectral information and improves spatial resolution considerably. As for the fused image by DFrFT, its spectral and spatial performances are both inferior to the DFRNT method.

Performances of these algorithms are further evaluated using objective quantitative assessment. Spectral and spatial performances are evaluated using two sets of criteria. Spectral quality of each fused image band is measured by spectral discrepancy (SPD), correlation coefficient (CC), and spectral angle mapper (SAM). At each band, SPD function can be written as

$$\mathrm{SPD} = \frac{\sum_{r,c} |M_{\mathrm{F}}(r,c) - M_{\mathrm{R}}(r,c)|}{N \times N}, \quad (14)$$

where $M_{\mathrm{F}}(r,c)$ and $M_{\mathrm{R}}(r,c)$ denote pixel values of fused and reference images at position (r,c), respectively. The Wald protocol[9] is applied to compare performance at the degraded scale. The original MS image at the resolution of 30 m is utilized as reference image M_{R}. Fused image M_{F} (30 m) is obtained by fusing the degraded MS (90 m) and Pan images (30 m). Based on M_{F} and M_{R} at degraded scale, SPD is computed. A small SPD indicates sound spectral performance.

CC describes the correlation degree between two images:

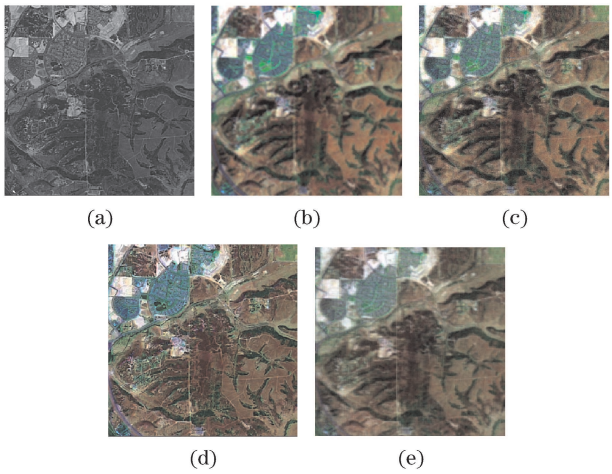

Fig. 2. Experiment on TM and SPOT Pan images. (a) Pan image; (b) re-sampled MS image; (c) fused image by DFRNT; (d) fused image by IHS; and (e) fused image by DFrFT.

Table 1. Performance Evaluation of Different Fusion Methods

Method	Band	CC	SPD	SAM	AG	Q_{avg}
DFRNT	R	0.9498	13.6822	9.1233	30.8028	0.8739
	G	0.9564	12.9445	9.5021	28.8842	
	B	0.9675	9.9896	9.4667	23.4601	
IHS	R	0.7896	25.2695	18.5662	37.1020	0.6536
	G	0.8260	22.6747	19.0140	34.0482	
	B	0.8894	16.5539	17.6773	26.5604	
DFrFT	R	0.8968	18.2322	12.8715	19.1379	0.8657
	G	0.9469	12.9880	10.3967	17.8924	
	B	0.9725	8.1356	8.6837	15.5594	

$$\mathrm{CC}=\frac{\sum_{r=1}^{N}\sum_{c=1}^{N}[M_{\mathrm{F}}(r,c)-\mu_{M_{\mathrm{F}}}][M_{\mathrm{R}}(r,c)-\mu_{M_{\mathrm{R}}}]}{\sqrt{\sum_{r=1}^{N}\sum_{c=1}^{N}[M_{\mathrm{F}}(r,c)-\mu_{M_{\mathrm{F}}}]^2\sum_{r=1}^{N}\sum_{c=1}^{N}[M_{\mathrm{R}}(r,c)-\mu_{M_{\mathrm{R}}}]^2}},\tag{15}$$

where $\mu_{M_{\mathrm{F}}}$ and $\mu_{M_{\mathrm{R}}}$ are the mean intensities of M_{F} and M_{R}, respectively. CC actually depicts the spectral information kept degree of the fused image compared with the original MS image. The ideal CC value is 1.

The SAM[10] describing the absolute value of spectral angle between two vectors is defined as

$$\mathrm{SAM}=\arccos\frac{\sum_{m=1}^{M}\boldsymbol{s}_m\boldsymbol{p}_m}{\sqrt{\sum_{m=1}^{M}(\boldsymbol{s}_m)^2}\cdot\sqrt{\sum_{m=1}^{M}(\boldsymbol{p}_m)^2}},\tag{16}$$

where $\boldsymbol{s}=(s_1,s_2,\cdots,s_M)$ and $\boldsymbol{p}=(p_1,p_2,\cdots,p_M)$ denote spectral vectors of each reference and fused band, respectively. SAM should be as close to zero as possible. The above indices only allow estimating the spectral difference between corresponding bands of the original and fused images. To estimate the global spectral quality, the following index is used.

$$Q_{\mathrm{avg}}=\frac{|\sigma_{\mathbf{z_1z_2}}|}{\sigma_{\mathbf{z_1}}\cdot\sigma_{\mathbf{z_2}}}\cdot\frac{2\sigma_{\mathbf{z_1}}\cdot\sigma_{\mathbf{z_2}}}{\sigma_{\mathbf{z_1}}^2+\sigma_{\mathbf{z_2}}^2}\cdot\frac{2\,|\overline{\mathbf{z_1}}|\cdot|\overline{\mathbf{z_2}}|}{|\overline{\mathbf{z_1}}|^2+|\overline{\mathbf{z_2}}|^2},\tag{17}$$

where Q_{avg} is a combination of three different factors[11], $\mathbf{z}_1=a_1+\mathbf{i}b_1+\mathbf{j}c_1+\mathbf{k}d_1$ and $\mathbf{z}_2=a_2+\mathbf{i}b_2+\mathbf{j}c_2+\mathbf{k}d_2$ denote pixel quaternion vectors for four-band reference and fused images, respectively. In the case of three components, as for color images, the quaternion's real part is usually set equal to zero[12]. Here, Q_{avg} is calculated using a 16×16 sliding window. The ideal value is 1.

For spatial quality, average gradient (AG) is employed. AG describes the changing features of image texture and detailed information. The larger the value of AG, the higher the spatial quality. AG can be computed by

$$\mathrm{AG}=\frac{1}{N\times N}\sum_{r=1}^{N}\sum_{c=1}^{N}\sqrt{\frac{\left[\frac{\partial M_{\mathrm{F}}(r,c)}{\partial r}\right]^2+\left[\frac{\partial M_{\mathrm{F}}(r,c)}{\partial c}\right]^2}{2}}.\tag{18}$$

Results of objective evaluation are listed in Table 1. It can be observed that spectral distortion introduced by the proposed DFRNT method is less than that based on IHS and DFrFT. This is attributed to random and uniform features of DFRNT spectrum distribution. As shown in Fig. 1, changes introduced by fusion produce a low influence on dispersed DFRNT spectrum, which is propitious to maintaining the spectral information. For DFrFT with centralized spectrum, changes introduce relatively strong spectral distortion.

Spatial performance of IHS method is superior to that of DFRNT. IHS method replaces the intensity component using the whole Pan image, which improves the spatial resolution considerably while severely distorting the spectral information of the MS image. While in principle based on the IHS transform, which usually only works for three bands, the proposed method is extended to any arbitrary number of spectral bands.

In conclusion, a new spectrum transform is introduced into the image fusion field and a novel fusion method based on DFRNT is proposed. DFRNT is a random transform with fractional order originating from DFrFT. In DFRNT transformed domain, high-amplitude and low-amplitude spectrum components, which take spectral information and spatial details, respectively, are extracted and fused with different fusion rules. The proposed method can properly preserve both spectral and high-resolution spatial information. Randomly and uniformly distributed spectrum makes changes by fusion random and dispersed. Thus, it has low spectral distortion. Its effectiveness is demonstrated with real TM and SPOT pan images. Furthermore, the feature of real output of DFRNT at half period can save storage space of image data, which is suitable for on-board processing.

This work was supported by the National Natural Science Foundation of China under Grant Nos. 10674038 and 10974039.

References

1. M. González-Audícana, J. L. Saleta, R. G. Catalán, and R. García, IEEE Trans. Geosci. Remote Sens. **42,** 1291 (2004).
2. D. L. Civco, Y. Wang, and J. A. Silander, in *Proceedings of ASPRS/ACSM Annual Convention and Exploration* **2,** 216 (1995).
3. J. Zhou, D. L. Civco, and J. A. Silander, Int. J. Remote Sens. **19,** 743 (1998).
4. Q. Zhang and B. Guo, Acta Opt. Sin. (in Chinese) **28,** 74 (2008).
5. C. Ye, Q. Miao, and B. Wang, Acta Opt. Sin. (in Chinese) **28,** 447 (2008).
6. M. Choi, R. Y. Kim, M.-R. Nam, and H. O. Kim, IEEE Geosci. Remote Sens. Lett. **2,** 136 (2005).
7. Z. Liu, H. Zhao, and S. Liu, Opt. Commun. **255,** 357 (2005).
8. S.-C. Pei and M.-H. Yeh, Opt. Lett. **22,** 1047 (1997).
9. L. Wald, T. Ranchin, and M. Mangolini, Photogram. Eng. Remote Sens. **63,** 691 (1997).
10. L. Alparone, S. Baronti, A. Garzelli, and F. Nencini, IEEE Trans. Geosci. Remote Sens. **42,** 2832 (2004).
11. L. Alparone, S. Baronti, A. Garzelli, and F. Nencini, IEEE Geosci. Remote Sens. Lett. **1,** 313 (2004).
12. S. J. Sangwine and T. A. Ell, IEE Proc.-Vis. Image Signal Process. **147,** 89 (2000).